Atmospheric Attenuation Correction and Ice Flag Algorithms for NSCAT

Simon H. Yueh, Wu-Yang Tsai, James N. Huddleston, Shu-Hsiang Lou, and Bijan Houshmand

Jet Propulsion Laboratory
California Institute of Technology
MS 300-235, 4800 Oak Grove Drive, Pasadena, CA 91109, USA
Tel: 818-354-3012, Fax: 818-393-.528.5, Email: simon@malibu.jpl.nasa.gov

Abstract This paper investigates atmospheric attenuation correction and ice flag algorithms for the NASA Scatterometer (N SCAT). The data from the Special Sensor Microwave/Imager (SSM/I) and SeaSat scatterometer (SASS) are analyzed to define and evaluate the applicability of potential algorithms. The results show that the monthly-averaged attenuation maps derived from the SSM/I data can be used to correct NSCAT data with a residual error of about (1.1 dB rms under rain-free conditions. However, when there is rain, the climatological attenuation map is not applicable because of the temporal and spatial variability of rain, and algorithms for rain flagging or correction remain to be investigated. NSCAT is designed to perform wind measurements over ice-free oceans. To reduce the temporal uncertainty of ice growth and motion, a sea-ice classification algorithm using the NSCAT data and the distinct physical scattering signatures of ocean surfaces and sea ice is proposed. This ice-flagging algorithm extends the performance of NSCAT into the polar oceans.

1. INTRODUCTION

Global ocean wind measurements are critical for ocean and atmospheric studies. NSCAT, the NASA Scatterometer [1], operates at Ku-band (13.995 GHz) and will be launched on the Japanese ADEOS-1 spacecraft in 1996 for the remote sensing of ocean winds. Ocean winds are the key driving force of atmospheric and ocean circulations. Each side of the swath with respect to the spacecraft ground track is illuminated by three antenna beams from different azimuth angles (Fig. 1). The fore and aft antenna beams are vertically polarized, while the middle beam is dual-polarized. The backscattered signals are Doppler-filtered using an on-board digital signal processor to produce 25 normalized radar cross-section (σ_0) cells simultaneously. The data collected from these three antenna beams allow the estimation of wind sped and direction based on the azimuth diversity of observation angles.

The electromagnetic waves at Ku-band frequency are more susceptible to attenuation from atmospheric cloud water and water vapor than at C-band, the operating frequency of the ERS-1 scatterometer. The atmospheric attenuation, if uncorrected, will degrade the performance of wind velocity measurements. Because there will be no companion microwave radiometers for atmospheric sensing on ADEOS-1, the use of other available remote sens-
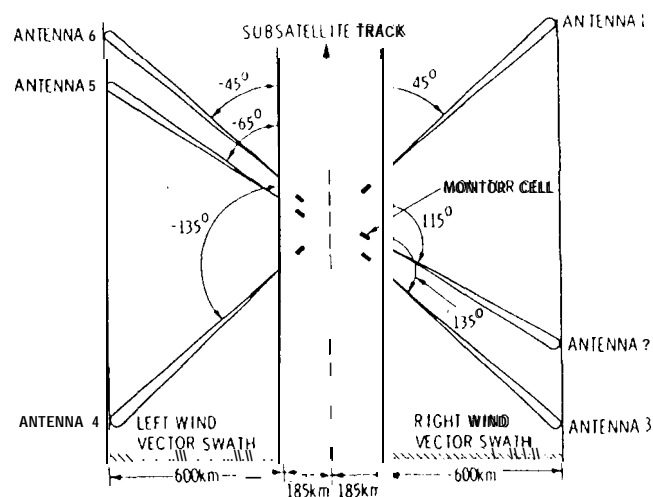

Figure 1 NSCAT Geometry

ing data sources needs to be considered for correcting the atmospheric attenuation. In addition, the lack of coincidental radiometer data requires an ice-flag algorithm which uses the scatterometer data to flag the presence of ice in the scatterometer footprint.

11. ATMOSPHERIC CORRECTION ALGORITHM

The data considered in this paper are from the Special Sensor Microwave/Imager (SSM/I), which is a multi-frequency scanning radiometer for the remote sensing of atmospheric parameters. The atmospheric attenuation dat a [2] derived from one year of SSM/I data have been analyzed. The geographical variations of attenuation data with or without rain were analyzed by grouping the data in 1° by 1° bins. The two-way atmospheric attenuation can reach as high as 0.6 dB without rain near tropical areas and becomes smaller for areas away from the equator. Data were also averaged on a monthly basis with the results indicating strong geographical and seasonal dependence, as illustrated in Fig. 2. The monthly standard deviations of atmospheric attenuation for all 1° by 1° cells were evaluated, indicating an average value of 0.1 dB under rain-free conditions and over 0.3 dB with all weather conditions considered. This means that under rain-free conditions, we can accurately correct for the atmospheric attenuation using the monthly-averaged attenuation map derived from the SSM /1 data. However,
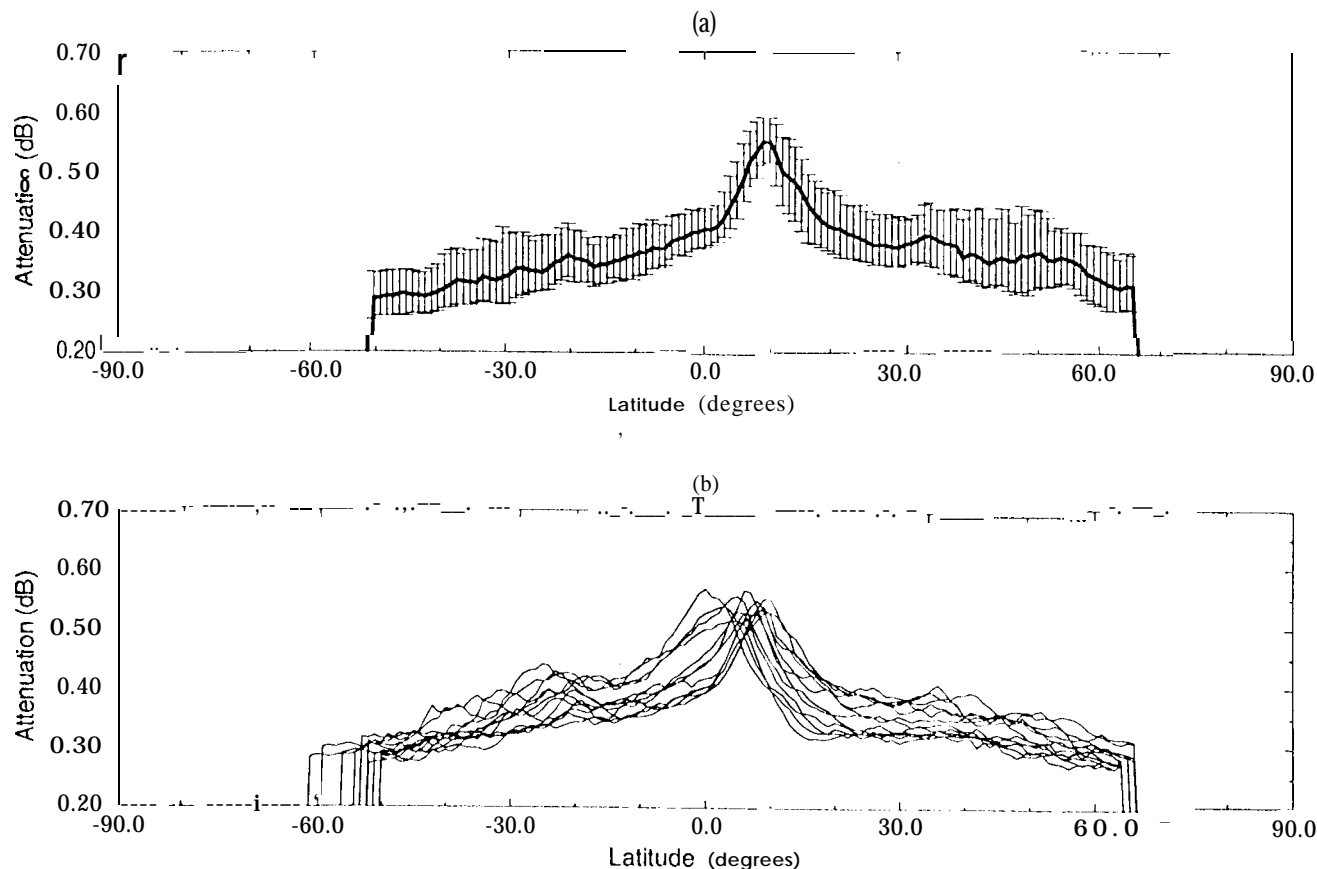
Figure 2. Two-way raill-free atmospheric attenuation versus latitude, longitude = -30°, incidence angle = 60° (a) Monthly average and ±1σ in July 1992. (b) Monthly average for 1992.

in the presence of rain there could be significant residual errors with this approach. Hence, further study on rain correction or flagging is required.

III. SEA ICE FLAGGING ALGORITHM

The ice flagging algorithm proposed uses the NSCAT data to distinguish between sea ice and wind-roughened ocean surfaces. This algorithm is based on the distinct scattering signatures of sea ice and ocean surfaces at moderate to large incidence angles [3], At small inci - dence angles, the radar backscattering is dominated by the rough surface, while at large incidence angles, it is dominated by volume scattering from brine inclusions and air bubbles in the ice. Because these volume scatter- ers have small ellipticities and arc randomly oriented in the azimuth direction, the co-polarized backscatter ratio $\gamma (= \sigma_{hh}/\sigma_{vv})$ for sea ice is close to unity at large inci- dence angles. In contrast, the Bragg scattering by cap- illary waves results in small γ at large incidence angles. Fig. 3 illustrates the co-polarized backscatter ratio from the sea ice and ocean surface as a function of incidence angles. It is shown that γ for sea ice is in general several dB larger than that of sea surfaces at low to moderate wind speeds at above 45 degree incidence angles. How-

ever, the difference reduces at higher wind speeds. To resolve the uncertainty in wind speeds, the absolute level of σ_0 is used to determine whether the wind speed is less than a certain value, such as 8 m/s. Fig. 4 illustrates the backscattering coefficients of sea ice aud sea surfaces as a function of incidence angles and shows that σ_{hh} of sea surface is less than -20 dB at an incidence angle greater than 45 degrees for 8 m/s winds.

Based on these observations, the NSCAT data col- lected by the dual-polarized antenna beams at greater than 50 degree incidence angles cau be confidently used to classify the ice and ocean for each pass. With the data collected from multiple passes, a continuous ice edge can be constructed using the collection] of fragmented ice edges obtained from every pass within a few days.

IV. SUMMARY

This paper presents algorithms for correcting the atmo- spheric attenuation under rill-free conditions and au ice- flagging algorithm for NSCAT. The proposed attenuation algorithm uses the monthly-averaged attenuation map derived from the SSM/I data. Although the performance of this algorithm in the absence of raio is acceptable, a u algorithm applicable to cells contaminated by rain
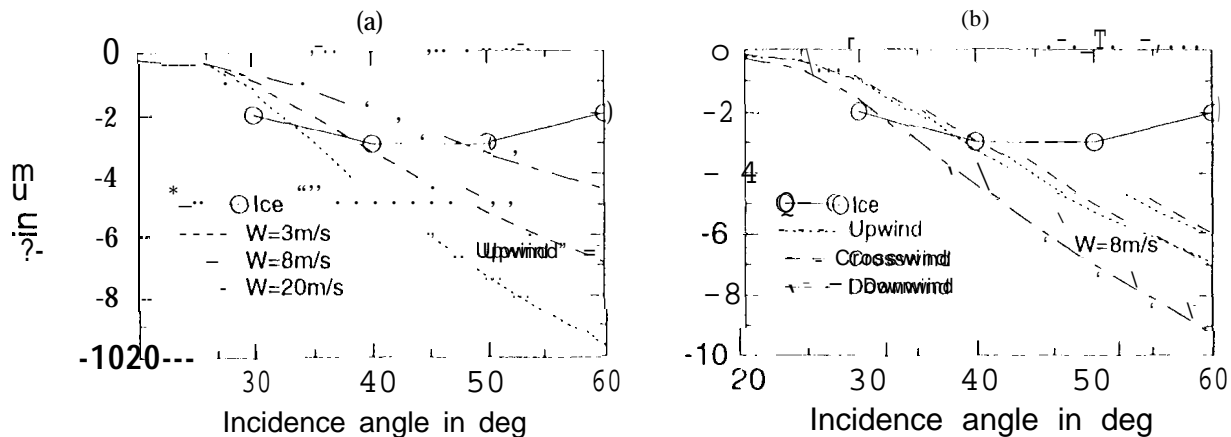
Figure 3. Copolarized backscatter ratio (γ) of first-year (FY) ice and wind-roughened sea surfaces as a function of incidence angles. σ_{hh} and σ_{vv} of the sea surface are calculated from Wentz's SASS geophysical model function [4]. σ_0 of FY ice was the backscatter data obtained by Kim et al. [5]. (a) Comparison of the copolarized ratio of ice and the sea surface at the upwind direction for three wind speeds. (b) Comparison of the copolarized ratio of ice and the sea surface at the up, cross, and down-wind direction for 8 m/s winds.
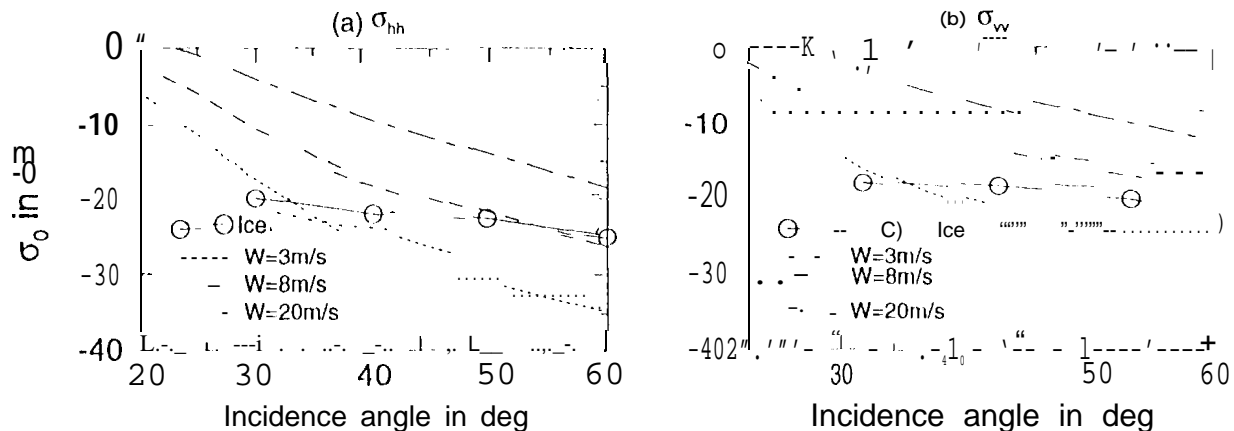

Figure 4. Backscattering coefficients **of first-year** (FY) ice and wind-roughened **sea** surfaces as a function of incidence angles. σ_0 of the sea surface is calculated from Wentz's SASS geophysical model function [4]. σ_0 of FY ice was the backscatter data obtained by Kim et al. [5]. (a) σ_{hh}, (b) σ_{vv}

remains to be determined. Finally, the approach of the Physical-based algorithm for ice flagging is described.

ACKNOWLEDGMENTS

REFERENCES

[1] Naderi, F. M., M. H. Freilich, and 1). G. Long, "Spaceborne Radar Measurement of Wind Velocity Over the Ocean - An **overview of the** NSCAT Scatterometer System," *Proc. of The IEEE*, Vol. 79, No. 6, 85(1--866, 1991.

[2] Wentz, F. J., "SSM/I derived atmospheric attenuation and rain rates for Sea Winds Scatterometer," Technical Report 051094, Remote Sensing Systems, Santa Rosa, CA, May 1994.

[3] Tsang, L., J. A. Kong, and R. T. Shin, Theory of Microwave Remote Sensing, Wiley-interscience, New York, 1985.

[4] Wentz, F. J., S. Peteherych, and 1,. A. Thomas, "A model function for ocean radar cross sections at 14.6 GHz," *J. G eophy. Res.*, Vol. 89, No. C3, 3689-3704, 1984.

[5] Kim, Y. S., R.K. Moore, and R.G.Onstott, "Theoretical and experimental study of radar backscatter from sea ice," RSL 'l'ethnical Report 331,37, Remote Sensing Lab., University of Kansas, Lawrence, 1984.